Chapter 11 – 3-D SEISMIC

Roger Hawthorne, Western Geophysical;

Ron Webster, Mobil Oil Canada

INTRODUCTION

If 2D seismic lines were acquired close enough together to exhibit spatial integrity in all directions, the equivalent of a 3D survey could be created (except for statics). Throughout most of the Western Canadian Basin, this limit of spatial integrity is 25 to 50 m. It is obvious that it would be very expensive and environmentally damaging to shoot such closely spaced conventional 2D seismic lines. With the recently-developed, large channel and multiline recording systems this spatial integrity can be achieved using surface lines separated by 8 or more times the distance of the required subsurface seismic line spacing. 3D seismic has become cost effective and feasible.

Prior to 1984 approximately 10 3D surveys had been shot in Canada. These were expensive and cumbersome to acquire. In 1984 multiline instruments were introduced and more than 20 surveys were recorded. The 3D method proved successful in delineating small stratigraphic targets and pinnacle reefs, and the number of 3D surveys more than tripled in 1985. Dispite the exploration downturn in 1986, the number doubled again and has increased annually. The number of 3D surveys in Canada in 1988 exceeded that of the rest of the world. Land surveys in Canada have tended to be small compared to much larger (100's km^2) marine surveys recorded elsewhere. The relatively small size of the Canadian surveys reflects the smaller physical size of the anomalies.

The interpretation advantages of 3D data are most important justification for their use. In this chapter, interpretational benefits are reviewed, reef examples shown, acquisition parameters are discussed, and a case history of a 3D survey in the Taber Area of Alberta is presented.

INTERPRETATIONAL ADVANTAGES

The example used to illustrate most of the interpretational advantages is from the Taber area, Alberta.

The most significant advantage of 3D seismic data is in the power of the 3D migration. To demonstrate this, a time window over the zone of interest on an east-west line has been selected from the center of the Taber 3D survey (Line 43, Fig.11.1). A significant difference is apparent between the migrated 2D and 3D sections. The main reason for the differences between the 2D and 3D migrated displays is that the seismic line is not perpendicular to the meandering river channel and cannot be correctly migrated on the 2D survey. Such data can be accurately migrated on the 3D data set. As evidenced by this example, all reservoirs are morphologically complex. It is, therefore difficult to select a line orientation which is perpendicular to the feature. 3D migration is the tool to insure spatial integrity.

The 3D survey technique gives a more accurate representation of the size and areal extent of features because of the denser spacing. This generally is at least a 20:1 ratio of lines per mile.

In Fig. 11.2 approximately every 20th line (400 m) is displayed. This line spacing would normally be considered detailed control for conventional 2D surveying. The geophysicist typically looks for features which are 10-20 traces in width. Often it can be difficult to relate features from line to line. Anomalies of one or two traces tend to be ignored because they could be due to noise, statics or multiples.

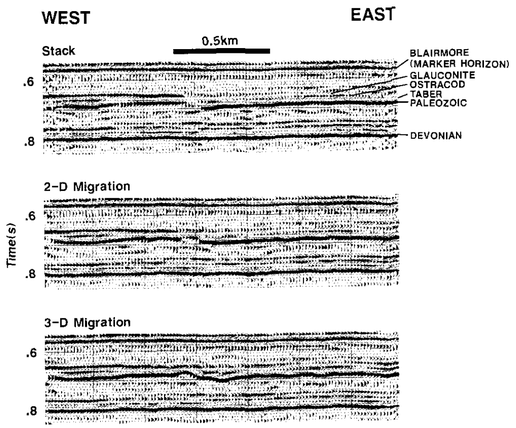

Figure 11.1. Window of data from the centre of a 3D land survey in the Taber area of Alberta. Note the significant, progressive change in the continuity and structure of the target event at 0.67 s from unmigrated stack to 2D migration, then from 2D to 3D migration. Such improvement in image detail is often just as dramatic for stratigraphic targets, as indicated here, as for structural ones.

Fig. 11.3, showing wavelet slices for lines 40-49 illustrates the close line control of a 3D survey with a line spacing, in this case, of 20 m. Line 40-49 represents a distance of only 180 m, which shows how quickly the geology changes. It is quite evident that the main events are a lot easier to follow from line to line but small features, as indicated by the arrows, of two to three traces also become possible to follow.

To further illustrate this point, a time slice is shown from the data volume flattened on the Blairmore. The time slice at 654 ms (Fig. 11.4) is approximately the middle of the Glauconite sandstones. This is an amplitude and polarity time slice and the sands tend to be the red shaded areas 'A' and 'B'. Note that a channel, 'C' cuts through the sands from about one-third the way down on the left side into the center and that another channel 'D' is evident from the upper right corner to the center of the figure. Channel 'C' is only 2-3 traces (40-60 m) wide but with the areal view of the 3D it becomes visible.

ACKNOWLEDGEMENTS

The author would like to thank Western Geophysical and Mobil Oil Canada for the information and interpretation of the Taber 3-D, and Western Geophysical for the use of the Joffree 3-D.

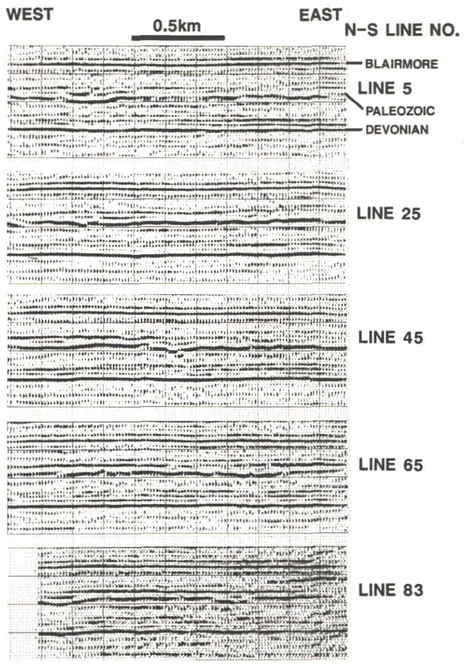

Figure 11.2. A window of data cut from every 20th line and placed one above the other so that the traces represent parallel subsurface positions every 400 metres. Note the change in geology from line to line.

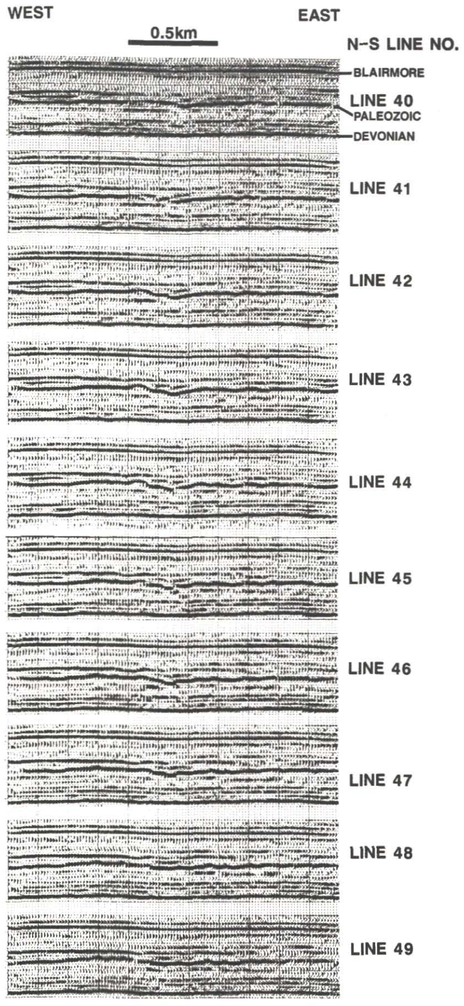

Figure 11.3. (Right) A window of data cut from lines 40-49, 20 metres apart. Note how rapidly the geology changes across the 180 metres.

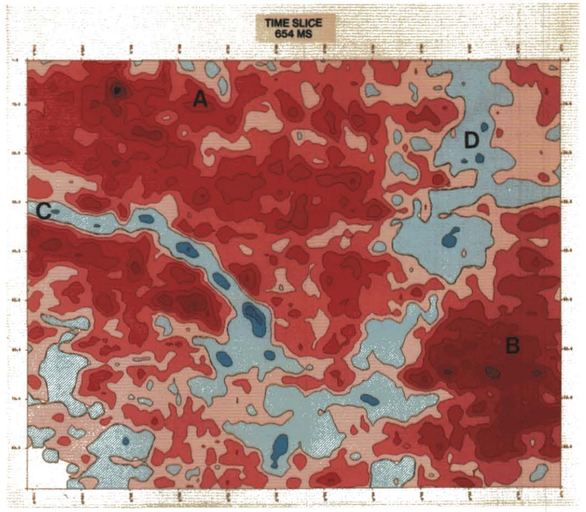

Figure 11.4. A time slice at 654 ms from a volume flattened on the Blairmore. Note that even 2 or 3 trace wide features such as the channel labeled "C" shows up readily.

WORKSTATIONS

Traditional methods of interpretation require geophysicists to examine each paper section, individually, and highlight horizons and faults with colored pencils. Then the interpreted values are posted onto a pre-specified map scale where the results are hand contoured. It has become apparent that traditional methods are not fast enough and that they do not extract all of the information in the large volumes of data associated with 3D seismic. Complementary advances in computer hardware and software have provided the tools whereby the geophysicist can manipulate large data volumes. These activities center around the concept of a geophysical workstation which several geophysicists can share.

A typical workstation (Fig. 11.5) allows the interpreter to display seismic data on high resolution color graphics screen and directly interpret these displays for 3D surveys. The following displays used in this example are from a 3D survey shot in the Joffre Area over the discovery well 15-22-39-26. The survey covered an area 2.4 by 4.02 kms with a cell size of 30 by 30 m to give 81 lines in a North-South direction and 135 lines in an East-West direction. It was shot with Vibroseis and with an average fold of 1500%. Typical displays which can be selected are portions of desired sections in the inline, crossline and time slice directions (Fig. 11.6A-C). Alternately, a loop or zigzag line can be developed through the data (Fig. 11.7A-B). Aside from the benefits of speed and convenience, workstations offer analytical tools that would not be available with traditional methods. For example, given a few guided points, most workstations can automatically track horizons ensuring that each interpreted pick is consistently on the same point of the seismic reflection. The workstation then presents the digitized results immediately on the screen for review and rapid manual editing. Not only is the time of the interpreted pick recorded but also the corresponding amplitude attribute (Fig. 11.8A-C).

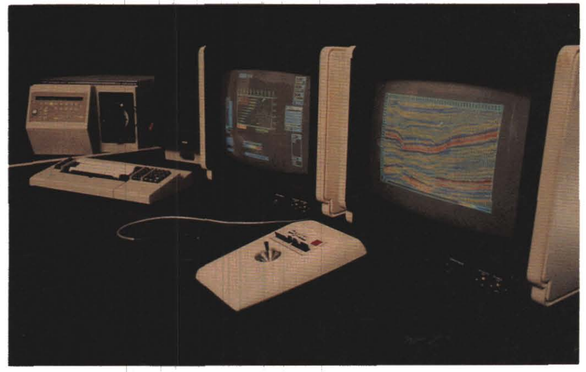

Figure 11.5. This workstation consists of two high resolution graphic screens, a terminal to communicate with the mainframe, a joystick for cursor positioning and also a hardware zoom feature, a digitizing pen for cursor control, and a camera with both polaroid and 35 mm capability which can create color slides or prints from either screen.

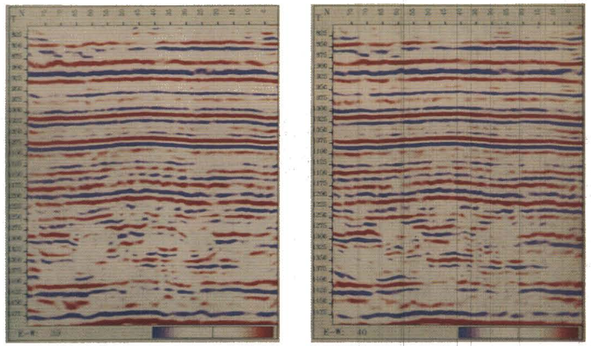

Figure 11.6a. The two inline sections displayed are across the 15-22 well. Crossline numbers are across the top and time down the side with inline numbers at the bottom. Interpreters select a horizon to be timed and give the workstation a few guide times which the station will correlate along the horizon, storing time, coordinates, amplitudes and frequency for later mapping uses. The picks can be passed to the next line for easy reference. A wide range of colors and trace displays are available. Most systems have both hardware and software zoom features to closely examine areas of interest.

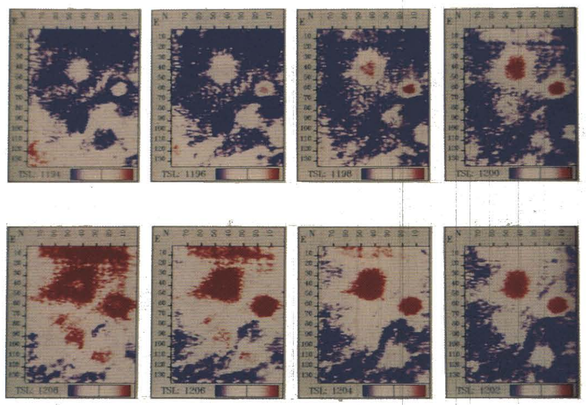

Figure 11.6b. (bottom left) Time slices taken from a time of 1194 to 1208 in two millisecond increments. The colors represent amplitude and polarity. The crossline numbers are on the side, inline numbers on the top of the time slice with the time slice time at the bottom. This type of display is useful in quickly viewing the size and movement of structure with increasing depth. TSL = time Slices.

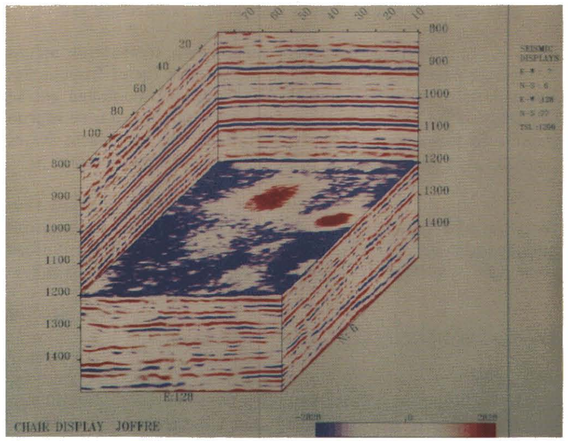

Figure 11.6c. Chair displays are useful to relate the time slices to the rest of the 3D cube by combining inline and crossline displays with the time slice. The corner coordinates are in a table to the right of the display.

Figure 11.7a. (above, top right) On the screen a map is used to originate the sections being interpreted. Well locations (in yellow) can be positioned on the map. Synthetics can also be stored with the well file to be displayed later with the data. The inline and crossline numbers are displayed along the side for easy reference and the red line is the line being displayed. The red numbers in brackets are the node points in the line which can be any shape.

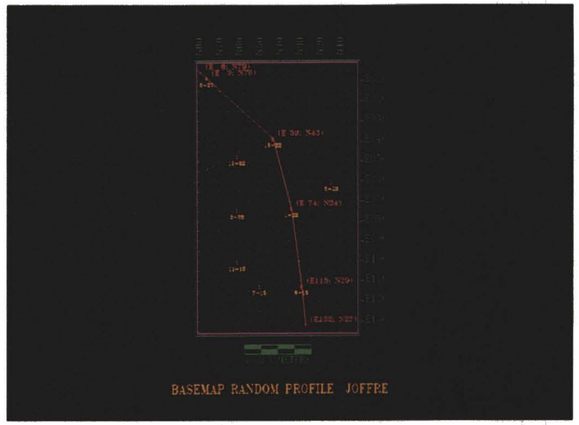

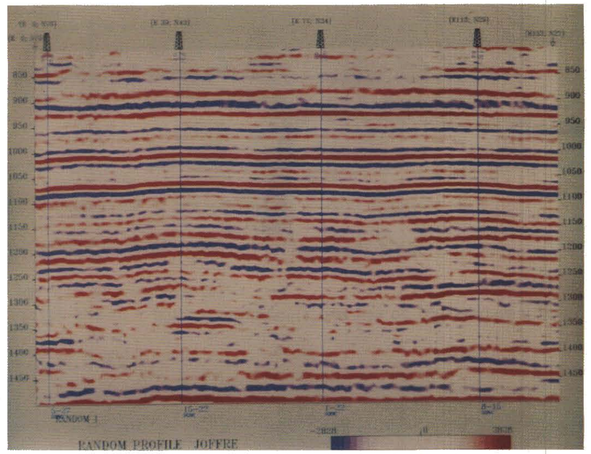

Figure 11.7b. This is the line derived from gathering data along the red line in Fig. 11.7a which goes through four wells. The crossline and inline coordinates are in black at the bends of the line, the well symbols are at the well locations with the well name at the bottom of the section and time down the side.

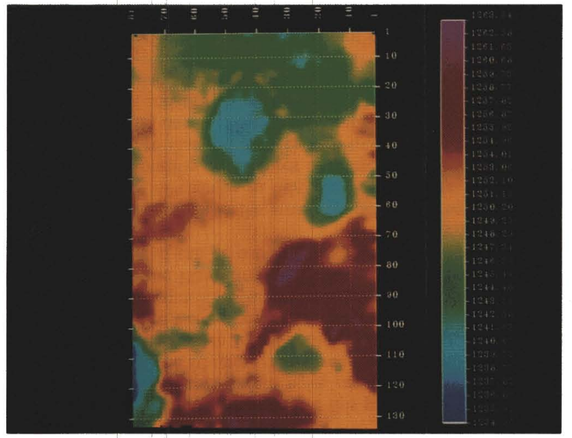

Figure 11.8a. Once the horizons are picked they can be displayed in many fashions. Past interpretations have usually resulted in contour maps. With the aid of color the highs and lows of the horizon can be quickly recognized. Isopachs from all interpreted horizons, may be calculated and displayed.

Workstations also present a host of utility options. Interpreters can request that well log and synthetic traces be superimposed on seismic displays and may interactively flatten selected horizons. As the interpretation proceeds, results can be directed to various hardcopy devices such as a plotter or camera. Connection with secondary packages such as modelling, mapping, vertical seismic profiles and amplitude versus offset analysis and other in-house database programs, increases the use and flexibility of workstations.

The advent of geophysical workstations has changed the day to day activities of geophysicists. Most workstations require only a few hours of instruction before the interpreter becomes familiar with the system. Geophysicists can now interpret data at least one order of magnitude faster than by hand. This increases the productivity of interpreters as well as allowing more time for comprehensive interpretations.

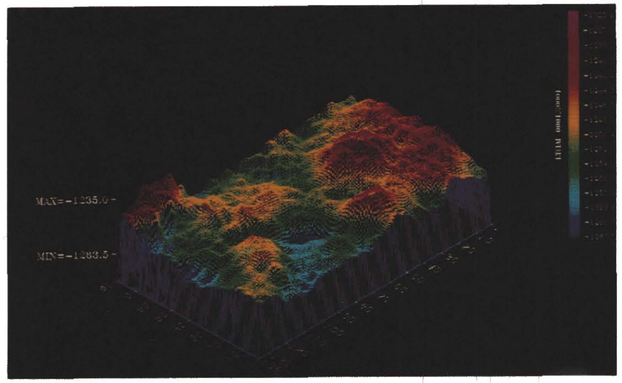

Figure 11.8b. As there is a time value for each point on the horizon a 3D view of the horizon can be built and viewed at any angle. The Ireton horizon is displayed in a net diagram with time color. It may also be useful to display the time in a net diagram and overlay the amplitude or frequency in color, thus allowing correlation of two attributes.

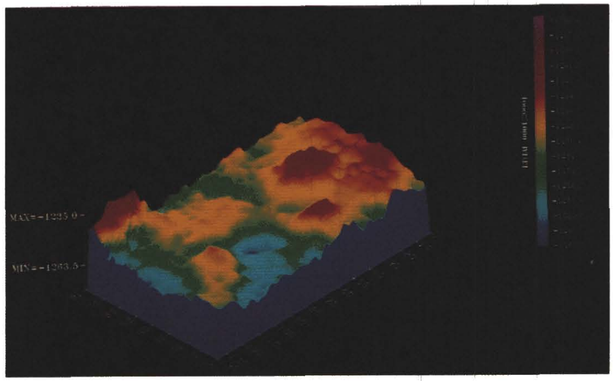

Figure 11.8c. The net may also be filled in with solid color. Inlines and crosslines are displayed at the bottom with the time scale on the left and a color versus time value at the right.

There is a well-documented, trend in computer hardware and software development permit time, performance and capabilities to go up while the price goes down. In the context of workstations this means desktop PC based systems capable of more geophysical operations will soon be available. In the near future, workstations will also have seismic data processing capabilities. Interpreters may then interactively correct for missties, change filters and gain parameters or devise entire processing sequences.

3D SURVEY DESIGN

The first step in acquiring a 3D program is to undertake a survey design. Economic restrictions and exploration goals have to be balanced.

It is not possible to present a single solution to a design problem. Each design must be tailored to a particular exploration goal to obtain the most suitable solution.

The main considerations are: 1) Survey Area; 2) Resolution Required; 3) Environmental Considerations; 4) Receiver Spreads and Shooting Sequences; 5) Instrumentation; 6) Impact of each on the Total Cost.

Survey Area

The overall surface size for a 3D seismic survey, must take into account the subsurface area of interest, regional and anomaly dips, proximity of the anomalies to the survey boundaries, and the area over which full multiplicity is required.

A migration aperture must be included around the edges of the survey to capture the energy that is diffracted outwards by anomalies or dips so it can be moved to the correct points on the time section by the migration algorithm. The migration distance required from the anomaly to the edge of the survey can be calculated by two simple formulae as stated below and illustrated (Fig.11.9)

Several estimates of parameters should be inserted into each equation. The largest value derived from each should then be used as the migration distance in a particular direction. Some typical values for Alberta are given in Fig. 11.10.

FORMULA 1

$X\ mig. = Z \sin$ = dip picked from unmigrated data

m = dip picked from migrated data

$X\ mig. = Z \tan m$ where Z = depth = $\frac{VrmsT}{2}$

X mig. = required distance

FORMULA 2

The size of a diffraction umbrella that will be collapsed to a point can also be computed by:

$$X\ mig. = \frac{Vrms}{2}\left[(Tm + \frac{1}{(2Fm)})^2 - Tm^2\right]\ 1/2$$

where Vrms = rms velocity to horizon of interst
Tm = max. 2-way time to horizon
Fm = min. frequency of interest

Figure 11.9. It is important to have the survey extend past the anomaly outline by the distance between the actual depth point and the assumed depth point to enable migration to properly represent the feature.

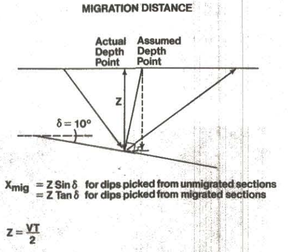

Figure 11.10. The intersection of the depth of the zone of interest along the top and the dip in degrees down the side will give the migration aperture in metres. These numbers are a useful guide but the migration distance should be calculated for each survey's needs taking into account the signal to noise ratio.

EXAMPLE MIGRATION DISTANCES

DIP (degrees) \ DEPTH (m)	1000	1200	1400	1600	1800	2000
5	87	105	122	139	157	174
10	174	208	243	278	313	347
15	259	311	362	414	466	517
20	342	410	479	547	616	684
25	423	507	592	676	761	845

The size of the feature being imaged dictates the area over which full multiplicity is required. Generally it takes between 4 and 8 cells (traces) to build up to full multiplicity from the edges of the survey. A migration aperture must also be considered but normally the low fold aperture can also be included in this distance although if the data has poor signal to noise ratio the migration aperture should be full fold.

Resolution Required

The resolution achieved on a 3D survey is dependent on the cell size, multiplicity, overburden thickness, surface noise and charge size.

The cell size is the 2-dimensional CDP interval over which data traces will be summed in the stacking process. Several concepts must be addressed in determining the best cell size for a survey. The maximum cell size for a given frequency and dip must be calculated to avoid spatial aliasing in the migration step. (Figure 11.11 a-c) The formula for the maximum spatial sampling interval is:

$$X_S = \frac{Vrms}{4\ Fmax \sin}$$

where Vmrs = rms velocity
Fmax = Max. frequency of event
X_S = cell spacing
= dip

Trace interpolation can help relieve this problem but its success depends upon adequate signal to noise ratio, wavelet character and the complexity of the structure. If desired to exceed the cell size by more than what the above formula allows trace interpolation may be used to help compensate, a test should be run on data across the structure before acquisition parameters are set. This is not a major consideration in the Plains area of Western Canada due to lack of extreme dips, but it can be a major factor in the Foothills.

Another consideration is the structural definition required by the spatial frequency of changes in lithology and structure. These changes usually outline the features of interest and therefore you want to make sure that you have enough traces to make a confident interpretation. 3D data provide the advantage of covering an anomaly areally and this strengthens the interpretation. This becomes evident upon examination of a time slice (Fig.11.13 a-c).

It is for this reason that one does do not normally need to use cell sizes on 3D data which are equivalent to CDP intervals on 2D data. Data that are oversampled are no better than data with a large but adequate cell size, but are much more expensive.

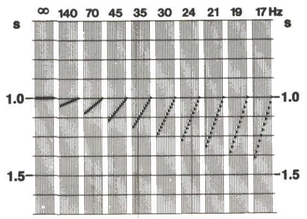

Figure 11.11a. Broadband (5 to 80 Hz) dipping events. For each dipping event, frequencies higher than those labelled above the dip segments are spatially aliased.

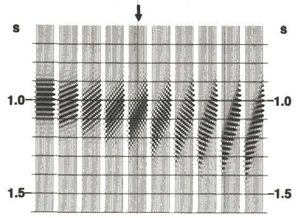

Figure 11.11b. Narrow bandpass filtering of the dipping events in Figure 11.11a (passband is 35-40 Hz). Events to the right of the arrow are spatially aliased. That is, the dips that the human observer (and computer) would interpret differ from the true dips as seen in Figure 11.11a.

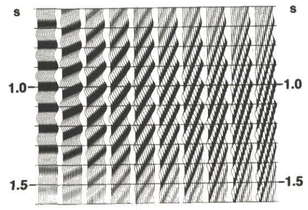

Figure 11.11c. Narrow bandpass filtering of the dipping events in Figure 11a (passband is 8.75-10 Hz). No frequencies within this passband are aliased, even for the most steeply dipping events. There is no difficulty in inferring the true dips of all the events.

Figure 11.13a. A hypothetical anomaly with erratic shape with an average width of 250 m.

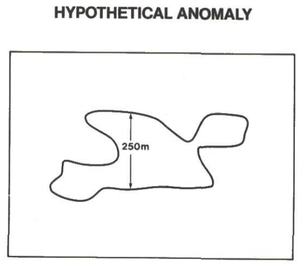

Figure 11.13b. The dashed line is the actual shape of the anomaly in Fig. 11.13a and the solid line is the shape if the center of each cell is used as a control point.

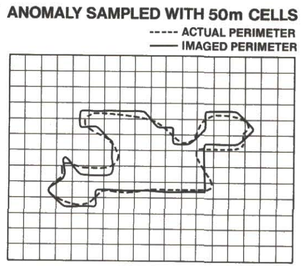

Figure 11.13c. Using the same basis as in Fig. 11.13b, it can be quickly seen that actual accuracy of the contour match is only slightly increased and yet there is a four to one increase in the number of cells. This might double the cost of the survey.

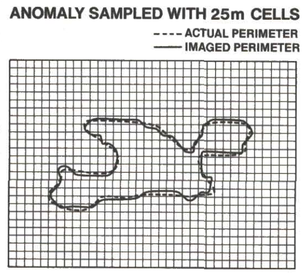

INSTRUMENTATION

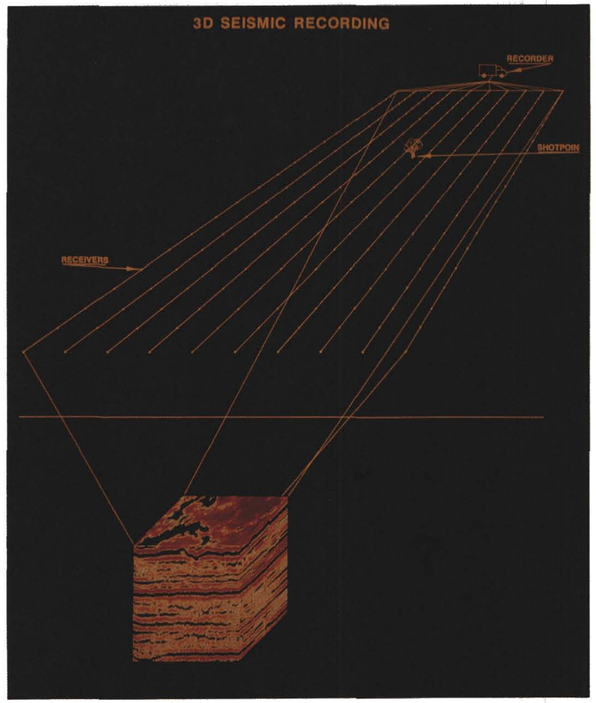

Typical multiline recording systems (above) generally feature more channels than conventional systems and provide the ability to record several lines at the same time. Being able to define spread parameters on each line independently has minimized costs on a 3D survey while offering maximum flexibility. There is a cut-off point for the number of channels that can be used at any one time. The main constraint is the maximum offset limit for the zone of interest. Monoline systems may be used for small surveys, but they limit the parameter choices greatly as one has to either use a crossed array where a single receiver line is crossed by many shot lines or one has *to snake the cable across several receiver lines. In this case, line* lengths must be such that the number of stations is an exact divisor of the number of channels, and a line must cross at the last station in order to connect the receiver lines together. In either case, the monoline approach is more cumbersome and time consuming for 3D work than the multiline systems.

COST DETERMINATION

The cost of a 3D survey is directly affected by many factors as shown in Fig.11.14. These factors are based on the particular

BLOCK DIAGRAM FOR COST DETERMINATION

Cost			Previous Seismic
Number, size & Depth of Shots	Number of Channels in Recording System	Target Depth ie. offset limits + Multiplicity Required	Well Logs & Isochrons
Amount of Line Work	Cell Size	+	
Number of Data Cells to Process		Lateral Resolution Required ie. size of anomaly	
Amount of Recording Time	Survey Area		
		Line Spacing ie. Forestry regulations	Existing Cut Lines
		+	
		Area of Interest	Anomaly Dips
		+	Regional Dips
		Migration Distance	Anomaly Location W.R.T. Boundaries
		+	
		Mineral Rights Ownership	
= Determined by			

Figure 11.14. Block diagram showing relationship of parameter selection to cost of the survey.

exploration problems, the resolution demanded, and "reasonable cost". Some of these factors are interdependent with more than one other factor, eg. number of shots, multiplicity, cell size, line spacing. The relationships become obvious when one actually considers which is the most important for a particular application based on pre-existing information such as previous seismic data, well logs, known dips, anomaly location, existing cut line and forestry regulations. The best way to view the relationships is of course to design a 3D survey, with appropriate weighting on the different factors.

Many of the basic factors involved with designing a 3D survey such as hole depth and charge size, are also common to 2D surveys. However, there is much more to consider to ensure the geophysical and economic integrity of 2 and 3D survey.

3D CASE HISTORY

The Taber area of Southern Alberta is characterized by rapid lateral facies changes within the Glauconitic Sandstone of the Upper Mannville Group (Lower Cretaceous). The reservoirs are sandstones with porosities of about 15%, surrounded irregularly by impermeable siltstones. A generalized and widely accepted interpretation of the geology in this area (Hradsky and Griffin, 1984) is shown in Fig. 11.15. Glauconitic Sandstone reservoirs are related to the main channel of an old river valley about 50 km long, 3 km wide, and up to 40 m deep. The valley crosses the area from northwest to southeast, dipping at about 5 m per km.

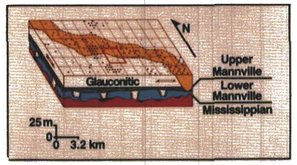

Figure 11.15. A postulated interpretation of the geology of a river-channel zone in the Taber Area of Southern Alberta. Note the exaggeration of the vertical scale. In true scale, the river valley would look like a thin layer for the area under study (the rectangle outlined in red).

As is typical of river-channel sandstones, their configuration is highly variable, making detailed delineation by 2D seismic exploration extremely difficult, even with a rather dense network of lines. To improve the prospects for reservoir delineation, a 3D survey was conducted and 3D inversion interpretation of the data performed.

To meet requirements for detailed imaging, subsurface coverage was at a 20x20 m spacing. The survey, conducted in a series of overlapping, parallel swaths of eight receiver lines each, produced 111 stacked traces in the receiver direction and 88 in the crossline direction. This effort yielded CMP coverage (typically 12- to 16-fold) over a 2,200 x 1,740 m area.

Figure 11.16 is a base map of the 3D survey showing the locations of the older producing wells (C, D, E, and F) and dry wells (A and B). Well names are identified by letters to preserve confidentiality, while the alphabetic order represents the sequence in which the wells were drilled. Successful wells (G and H) were drilled after the 3D survey was acquired, while new producing wells (I and J) were drilled later after the inversion modeling study was completed.

Figure 11.16. 3D seismic survey area map with well and sample seismic traverse location.

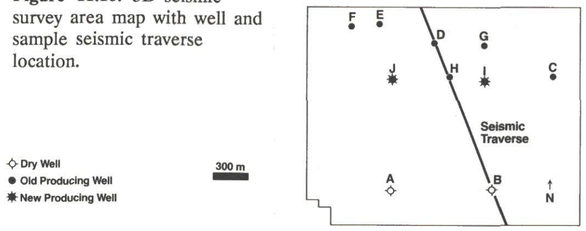

Historically, a major criterion in choosing drill sites in this area has been amplitude anomalies associated with the Glauconitic event (at about 650 ms). The sandstone reservoirs give rise to an approximate 30% increase in amplitude relative to that associated with the siltstone facies (follow, for example, the trough at 650 ms in Fig. 11.17). Despite the subtlety of the available criteria for interpretation, production has been predicted with considerable success: four producing wells out of six locations within the area of the 3D survey. 3D inversion modeling interpretation of the data was undertaken to improve on this success ratio. Specified goals were to enhance the temporal resolution required to delineate the sands and to quantify estimates of reservoir parameters such as gross pore volume and reserves in place.

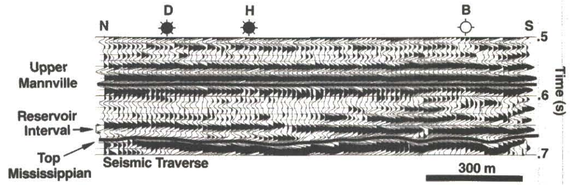

Figure 11.17. Line 28 of the Taber 3D survey flattened on the Blairmore.

This modeling procedure produces a thin-layer, highly resolved velocity model from bandlimited, noise-contaminated seismic input data by simulating the interference effects of closely spaced reflectors. When applied to properly conditioned seismic data, this forward modeling technique also is comparatively insensitive to random noise. This is because the 2D process searches for lateral continuity of model layers, rather than aiming for a perfect match between the synthetic seismogram and the recorded seismic traces. The user-controlled bedding geometry input to the program required only a general velocity model, with layer thicknesses typically on the order of 300 m or 200 ms (milliseconds). In contrast, the output model provides a thin-layer solution (Fig. 11.18) whose synthetic response is consistent with the recorded seismic data along a traverse joining producing wells D and H and dry well B (Fig. 11.17). The interpreted markers on Figure 17 define the coarse three-layer input model supplied for the lithologic modeling, with interval velocities of 2800, 3500, and 5200 m/s, from top to bottom.

The derived thin-layer velocity model reveals details of the reservoir stratigraphy approximately 190 m below sea level (or 980 m below ground level). The Glauconitic reservoir sandstone, which produced at wells D and H in the north, is truncated to the south by a higher velocity silt-filled channel, where dry well B was drilled (Fig. 11.18).

The inversion results show distinct lateral and vertical changes in layer velocity. For example, the Glauconitic Sandstone target zone appears as a thin (0-40 m) layer with velocities ranging from 3,200 m/s (very porous sand to 4,000 m/s (impermeable siltstone).

Although this 3D survey is not large, each of the derived 3D volumes (velocity model and synthetic data) contained more than

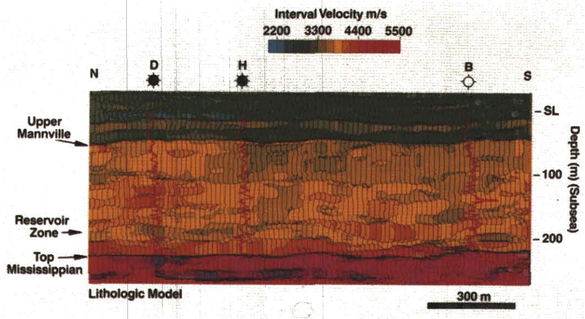

Figure 11.18. Velocity-depth model from seismic modelling showing erosional truncation of reservoir sand and overlay of sonic logs.

9,000 traces. An interactive interpretation system was used in the analysis of the 3D inversion interpretation. Most of the figures of 3D inversion results for the Taber 3D survey shown here, were generated on the interactive interpretation system.

Fig. 11.19, 20 and 21 show isometric displays of the 3D seismic data, the resulting 3D synthetic data, and the inversion derived 3D velocity model. The patterns seen on the time slices of the field and synthetic seismic data are similar. These patterns, however, are not recognizable in the corresponding time slice of the velocity model. It should be noted that the synthetic data are obtained directly from the derived inversion model and are also consistent with the seismic data. In extending the level of detail beyond that perceived directly in the seismic data the inversion results can change the interpretation. For example, study of the seismic data alone might lead one to interpret the narrow red traverse of negative amplitudes in the time slice at 652 ms shown in Fig. 11.19 as the deepest (and assumed thickest) part of the river valley. The derived velocity model, however indicates that this feature may not be a channel at all; instead, it may be related to an abrupt decrease of the sandstone/siltstone ratio in the layer of interest. The apparent discrepancy between the patterns in the data and that in the model can be attributed to the band limitation of the data. Features seen on a given time slice will have been influenced by positions of the (broadband) model at nearby levels.

Figure 11.19. 3D seismic data cube. The top slice is at 652 ms (near the top of the Glauconitic Sandstone within the area under study). Color denotes relative seismic amplitude (blue denotes strong positive amplitude and red denotes strong negative amplitude).

Figure 11.20. 3D final synthetic seismic data cube. The top slice is at the same level (652 ms) as that in Fig. 11.19. The average crosscorrelation coefficient between these data and the field-derived data (Fig. 11.19) is 0.93. The color scheme is the same as that in Fig. 11.19.

Figure 11.21. 3D final velocity-time model. The time slice is again at 652 ms. Note that the (broadband) inversion interpretation here is not obvious from visual analysis of the (band-limited) seismic data (Fig. 11.19) despite the good match between the synthetic and the data. The color scale represents velocity. Within the Glauconitic Sandstone, red and yellow are indicative of low-velocity, porous sands.

Figure 11.22. 3D velocity-depth model in the vicinity of borehole C. This well is a gas and oil producer. Yellow and red in the Glauconitic Sandstone are indicative of reservoir sands.

Figure 11.23. 3D velocity-depth model cut so as to show oil producing boreholes E and F along the front section.

Figure 11.24. 3D velocity-depth model showing dry holes A and B along the front section. Well A has no show of sand (yellow) at the level of the Glauconitic Sandstone. Borehole B penetrates a narrow high-velocity zone.

Figure 11.25. 3D velocity-depth model. A new oil producer, borehole G (Fig. 11.16). The inversion interpretation indicates low velocity sand at the borehole.

Figure 11.26. 3D velocity-depth model. Another new oil producer, borehole H (Fig. 11.16). The inversion interpretation suggests low-velocity sand at this location also.

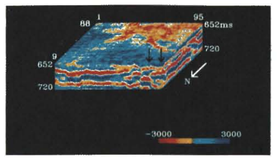

FIG. 19

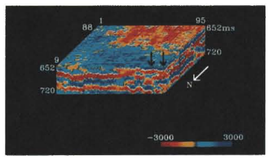

FIG. 20

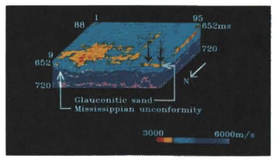

FIG. 21

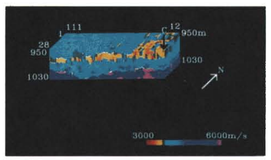

FIG. 22

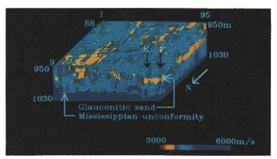

FIG. 23

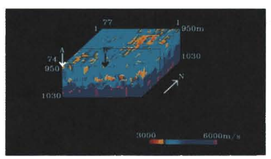

FIG. 24

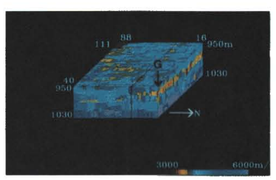

FIG. 25

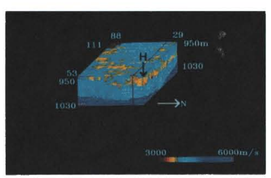

FIG. 26

Although the initial model was built on the basis of the sonic log from only one of the boreholes (borehole C), the derived inversion velocity solution is consistent with the log information from all six boreholes drilled within the study area (boreholes A through F in Fig. 11.16). Fig. 11.22 shows the inversion results in an isometric view that best displays the Glauconitic Sandstone in the vicinity of well C, the one used for calibration of the parameters in the initial model. The result shown in this 3D perspective no longer yields the irregular appearance seen in Fig. 11.18b; the Glauconitic Sandstone becomes a definite layer, but one with rapid variations of layer velocity attributable to variations of lithology from porous sandstones to impermeable siltstones. As the inversion model indicates, the well (A producer) penetrates the low-velocity porous sandstones of the Glauconitic Sandstone.

Fig. 11.23 shows two more producing wells that penetrate the Glauconitic Sandstone where the inversion interpretation again indicates porous sandstone. Fig. 11.24, in contrast, shows two dry holes. One of them, well A, was drilled through siltstone at a place where the inversion model shows high velocity. The second dry hole, well B, was drilled in what appears to be a narrow high-velocity zone beyond the resolution of the inversion processing.

Two additional wells were drilled within the survey area after the inversion and based on the data interpretation was made. Both of them are oil producers (wells G and H in Fig. 11.16). The inversion interpretation in the vicinity of those wells is shown in Fig. 11.25 and 26.

CONCLUSION

The 3D Seismic Imaging Approach to exploration is an oil industry standard, both in exploration and production applications.

Users of the technique must pay particular attention to initial parameter selection to ensure survey objectives are met. Some basic considerations have been addressed in this chapter: However, consultation with people experienced in survey design is recommended.

3D surveys will almost certainly be commonplace in the future to aid geologists, geophysicists and engineers in the imaging of such diverse targets as enhanced oil recovery projects, oil sands development, and coal and potash mines.

REFERENCES

DeBuyl, M. and Guidish, T., 1986. "The Reliability of Seismically Derived Reservoir Parameters, a Case Study in the Taber Turin, Alberta, Canada": paper presented at the Canadian Society of Exploration Geophysicists Annual Meeting, Calgary, Alberta.

Gelfand, V. and Larner, K. 1984. Seismic Lithologic Modeling: The Leading Edge, 3 p. 30-35.

Gelfand, V., Taylor,G., Tessman, J., and Larner, K., 1985. "3-D Seismic Lithological Modeling to Delineate Rapidly Changing Reservoir Facies, Case History from Alberta": paper presented at 55th Society of Exploration Geophysicists Annual Meeting, Washington, D.C.

Hawthorne, Roger, May 1985. "Other Benefits of 3D", paper presented at Canadian Society of Exploration Geophysicists convention.

Hawthorne, Roger, August 1985. "Acquisition and Processing Benefits of 3D Seismic", paper presented at Society of Economic Paleontologists and Mineralogists convention Golden, Colorado.

Hopkins, J.C., Hermanson, S.W., and Lawton, D.C. 1982. Morphology of Channel and Channel Sand Bodies in the Glauconitic Sandstone Member (upper Manniville), Little Bow Area, Alberta"; Bull. Can. Pet. Geol., 30,4, p. 274-285.

Hradsky, M. and Griffin, M. 1984. Sandstone Body Geometry, Reservoir Quality and Hydrocarbon Trapping Mechanisms in the Lower Cretaceous Manniville Group Taber/Turin Area, Southern Alberta; Cdn. Soc. of Petrol. Geol., Memoir 9, p. 401-411.

Larner, Ken, 1980. Trace Interpolation, Western Geophysical.

SEG Leading Edge, August 1986. Geophysical Activity Rpt, p. 25-48.

SEG Leading Edge, August 1987. Geophysical Activity Rpt, p. 25-49.

SEG Leading Edge, August 1988. Geophysical Activity Rpt, p. 33-56.

West, Mike, May 1985. "Design Considerations for 3D Seismic Acquisition in Western Canada", paper presented at Canadian Society of Exploration Geophysicists convention.